processes

MDPI

Article

Stability of Combined Continuous Granulation and Agglomeration Processes in a Fluidized Bed with Sieve-Mill-Recycle

Eric Otto [1,*], Robert Dürr [2] and Achim Kienle [1,3]

[1] Automation/Modelling, Otto von Guericke University Magdeburg, Universitätsplatz 2, 39106 Magdeburg, Germany
[2] Engineering Mathematics, Magdeburg-Stendal University of Applied Sciences, Breitscheidstraße 2, 39114 Magdeburg, Germany
[3] Process Synthesis and Process Dynamics, Max Planck Institute for Dynamics of Complex Technical Systems, Sandtorstrasse 1, 39106 Magdeburg, Germany
* Correspondence: eric.otto@ovgu.de

Abstract: Particle formation in fluidized beds is widely applied in an industrial context for the solidification of liquids and size enlargement of granular materials. The two main size-enlargement mechanisms are layering growth and agglomeration. For continuous process configurations with sieve-mill-recycle and layering growth only, the occurrence of undesired self-sustained oscillations in the particle size distribution under certain process conditions is well-known. This contribution investigates the stability of the practically relevant process with additional particle agglomeration by means of a model-based numerical bifurcation analysis. It is shown that the occurrence of stable limit cycles is inhibited by an increased rate of particle agglomeration for a variety of different process conditions and different agglomeration kinetics. These results enhance the understanding of the agglomeration and layering growth dynamics and are relevant for the process design and operation.

Keywords: fluidized bed; granulation; agglomeration; layering growth; bifurcation analysis

Citation: Otto, E.; Dürr, R.; Kienle, A. Stability of Combined Continuous Granulation and Agglomeration Processes in a Fluidized Bed with Sieve-Mill-Recycle. *Processes* **2023**, *11*, 473. https://doi.org/10.3390/pr11020473

Received: 14 December 2022
Revised: 31 January 2023
Accepted: 1 February 2023
Published: 4 February 2023

1. Introduction

Agglomeration and layering growth in fluidized beds are efficient particle formulation and size enlargement processes for solid materials, due to good particle mixing and high mass and energy transfer rates. The possibility to influence product particle properties such as size and porosity directly by a variety of different process variables [1] and create a high-quality product is important from an industrial point of view. Therefore, these processes are applied widely for the production of agricultural, chemical, pharmaceutical and food products such as fertilizers, milk powder and fine chemicals. In the layering growth process a solution is sprayed continuously on the surface of the fluidized particles. After the solvent has dried a new solid layer remains whereby the particle size increases slowly during the course of the process and an onion-like structure is formed as presented schematically in Figure 1. In contrast to this the size of the particles increases rapidly due to agglomeration of particles. When two wet particles collide in the turbulent fluidization air stream, there is a chance of aggregation due to viscous and capillary forces acting between the wet surfaces [2]. After the drying of the solution a solid connection between the two particles is formed as pictured in Figure 2. Layering growth is usually applied for the solidification of wet materials while agglomeration is desired if the size of particles has to be increased quickly, however depending on the process configuration and setting of process parameters both subprocesses can occur simultaneously [2,3].

For large scale production, these processes are operated continuously and often equipped with a sieve-mill cycle which serves for the separation, grinding and recycling of oversized particles. This configuration is more economic due to the reuse of the

oversized particles. However, the recycle may also introduce instability in the form of self-sustained oscillations. These have been reported for layering growth in simulation studies of well-mixed process models [4,5] and models with zone-formation [6] and confirmed experimentally [5,7,8]. In all of the latter contributions porous sodium benzoate particles were produced over the course of 25 and 36 h respectively resulting in undamped oscillations of the mean particle size between the milled particle size and a maximal value. From a practical point of view such oscillations have to be avoided for a stable process operation by choosing proper process parameters or by implementing stabilizing process control methods [9–11]. The occurrence of oscillations is mainly related to the size of the milled particles (or the milling grade) and also seems to be a result of the control of the total bed mass [12] which, however, is indispensable from the operational point of view. In fluidized bed configurations where agglomeration is the dominant size enlargement mechanism stable oscillations have not been observed to the best knowledge of the authors. The question regarding processes where both size enlargement mechanisms occur has been investigated by the authors in the conference contribution Otto et al. [13] by means of numerical bifurcation analysis. It has been shown in different simulation scenarios, that generally, shifting size enlargement from pure layering growth to agglomeration, tends to dampen oscillations and stabilize the whole process. The aim of the present contribution is to give a more detailed description of the underlying process model, to extend the previous results to a larger set of bifurcation parameters and give explanations of the observed phenomena.

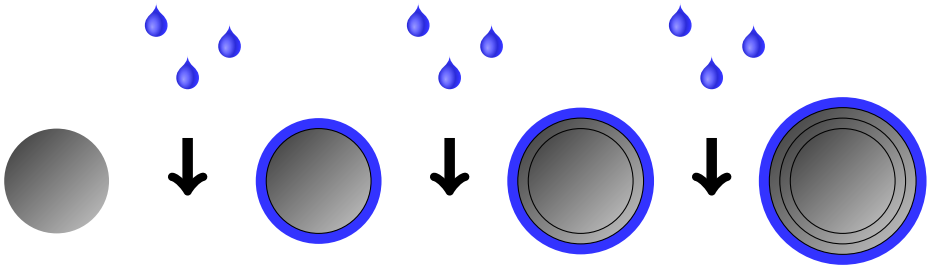

Figure 1. Layering growth subprocess resulting in an onion-like particle structure.

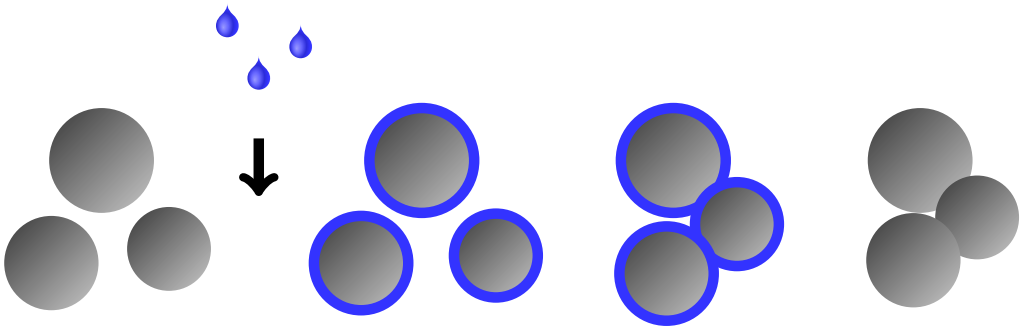

Figure 2. Agglomeration subprocess resulting in a blueberry-like particle structure.

The second and third section are concerned with the description of the population balance process model and the parameter bifurcation algorithm, respectively. The contribution concludes with the presentation and discussion of bifurcation plots for various parameters in the fourth chapter and a short summary in section five.

2. Process Model

In this contribution a plant configuration with sieve-mill-recycle is investigated where particles are added to and withdrawn continuously from the fluidization chamber. The withdrawn particles are separated into three fractions by two sieves. Particles meeting the desired product size specification are withdrawn while oversized particles are milled and

re-fed to the process chamber together with the undersized fraction. A schematic representation of the plant with an additional external particle feed is presented schematically in Figure 3.

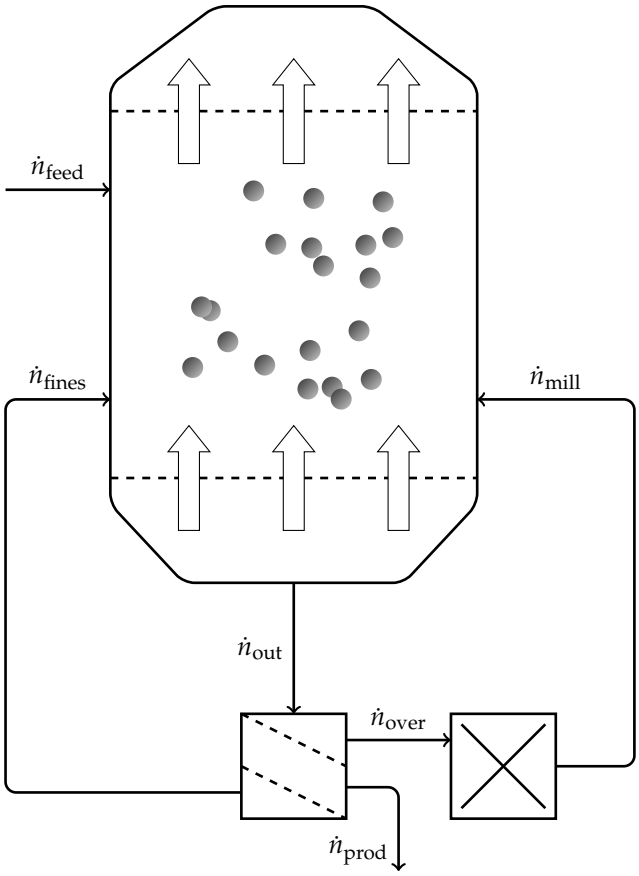

Figure 3. Schematic representation of the process chamber and periphery. Particles are fluidized in the chamber by an upwards facing air stream. Particles are withdrawn ($\dot{n}_{\text{out}}$) and sieved into three fractions ($\dot{n}_{\text{over}}$, $\dot{n}_{\text{prod}}$, $\dot{n}_{\text{fines}}$). The latter ones are feed back to the fluidization chamber and feed particles are added. The product particles are removed from the process while oversized particles are milled and then fed back to the fluidization chamber ($\dot{n}_{\text{mill}}$).

A well-established framework for the mathematical description of agglomeration and layering growth processes is population balance modeling [14]. Here the evolution of a particle population, distributed with respect to some internal or external properties x, such as size, shape or spatial coordinates, is described by a nonlinear partial differential equation, the so-called population balance equation (PBE). The current state of the population is given by the number density function (NDF) $n(t, x)$, describing the number of particles at time t in the infinitesimal interval $(x, x + \mathrm{d}x)$ of the internal coordinates. For well-mixed systems such as fluidized beds it is reasonable to assume that there are no spatial gradients in the bed, therefore spatial coordinates can be neglected. An important internal granule property is the characteristic size, since many other important properties such as the angle of repose or the porosity are correlated to it. In fluidized bed processes it is convenient to assume that all particles are spherical, thus their respective size can be characterized by either the particle diameter L or the according volume v, given by

$$v = \frac{\pi}{6} L^3. \tag{1}$$

While layering growth is most commonly described in terms of the particle diameter [15–17], the agglomeration term is predominantly given with respect to the volume

coordinate [14,18]. In the present contribution we choose to transform the layering growth term and model the complete PBE in volume coordinates, i.e., $x = v$ and $n = n(t, v)$. The solution of the agglomeration term requires the application of efficient numerical techniques guaranteeing conservation of total mass and correct computation of particle number. For those approaches the description of the particle density with respect to particle volume is convenient, whereas the layering growth term can be discretized using a first-order upwind scheme regardless of the choice of the internal coordinate.

The PBE describing the evolution of $n(t, v)$ is obtained by balancing all the particles streams into and out of the fluidization chamber according to Figure 3 and adding sink and source terms reflecting layering growth and agglomeration, yielding

$$\frac{\mathrm{d}n}{\mathrm{d}t} = \dot{n}_{\mathrm{agg}} + \dot{n}_{\mathrm{growth}} + \dot{n}_{\mathrm{feed}} - \dot{n}_{\mathrm{out}} + \dot{n}_{\mathrm{fines}} + \dot{n}_{\mathrm{mill}}. \tag{2}$$

In the subsequent paragraphs the right-hand side terms of Equation (2) are described in detail in accordance with Radichkov et al. [4], Heinrich et al. [15] and Neugebauer et al. [5] as well as Otto et al. [13].

The diameter-based layering growth is described by the advection type equation

$$\dot{\tilde{n}}_{\mathrm{growth}}(t, L) = \frac{\partial \tilde{n}(t, L)}{\partial t} = -\tilde{G}\frac{\partial \tilde{n}(t, L)}{\partial L} \tag{3}$$

where $\tilde{G}$ with $\left[\tilde{G}\right] = \mathrm{m\,s^{-1}}$ describes the diameter-independent growth rate and is given by

$$\tilde{G} = \frac{\mathrm{d}L}{\mathrm{d}t} = \frac{2\dot{m}_{\mathrm{inj}}}{\rho A_{\mathrm{p}}} \tag{4}$$

which can be found e.g., in Heinrich et al. [15]. Here, $\dot{m}_{\mathrm{inj}}$ describes the injection rate of binder mass, ρ the binder density and A_{p} the total particle surface defined by

$$A_{\mathrm{p}} = 6^{2/3}\,\pi^{1/3}\int_0^{\infty} v^{2/3} n(v)\,\mathrm{d}v\,. \tag{5}$$

It is assumed that the binder solution is distributed uniformly on all particles and that the solvent evaporates completely. In order to transform Equation (4) to a volume-based formulation

$$\dot{n}_{\mathrm{growth}}(t, v) := \frac{\partial n(t, v)}{\partial t} = -G\frac{\partial n(t, v)}{\partial v}, \tag{6}$$

the volumetric growth rate G has to be computed from $\tilde{G}$ for which the relationships

$$\tilde{G} = \frac{\mathrm{d}L}{\mathrm{d}t}, \quad G = \frac{\mathrm{d}v}{\mathrm{d}t} = \frac{\mathrm{d}v}{\mathrm{d}L}\frac{\mathrm{d}L}{\mathrm{d}t} \tag{7}$$

as well as Equation (1) and (4) are utilized, resulting in

$$G = \pi\left(\frac{6v}{\pi}\right)^{2/3}\frac{\dot{m}_{\mathrm{inj}}}{\rho A_{\mathrm{p}}}. \tag{8}$$

Notably, the growth rate is inversely proportional to the total particle surface, resulting in slow particle growth for beds with high surface.

The particle size enlargement by agglomeration is modeled using the following integral terms

$$\dot{n}_{\mathrm{agg}} = \frac{1}{2}\int_0^{v} \beta(t, u, v-u) n(t, u) n(t, v-u)\,\mathrm{d}u - \int_0^{\infty} \beta(t, v, u) n(t, v) n(t, u)\,\mathrm{d}u\,, \tag{9}$$

where the first term on the right-hand side describes the 'birth' of new agglomerates due to coalescence and the second term describes the 'death' of the two parent parti-

cles [14,18]. The kinetic rate of this second order process is given by the agglomeration kernel $\beta(t, u, v-u)$ describing the rate of successful agglomeration events depending on the volume of the involved particles. Due to the complex interaction of different mechanical and thermodynamical micro-processes leading to the aggregation of two agglomerates, the function β depends on various process, plant and material parameters. For example, the viscosity of the binder affects the inter-particle forces during particle collision and the temperature of the fluidization medium affects the drying behavior of the binding agent on the particle surface and thereby the formation of solid bridges between the primary particles [1,2,19]. Hence, modeling of β is a challenging task with different approaches of varying complexity to be found in the literature [2,20–23]. In order to investigate the influence of different agglomeration kinetics on the stability and at the same time keep the model simple, the rather general kernel function

$$\beta(u, v) = \beta_0 \frac{(uv)^a}{(u+v)^b} \tag{10}$$

is applied in this contribution. With the free parameters a, b and β_0, the latter also called agglomeration efficiency, different shapes of the kernel function and hence different types of agglomeration kinetics can be approximated [24]. In the nominal case $a = b = 0$ the kernel function becomes $\beta(u, v,) = \beta_0$, corresponding to a volume-independent agglomeration rate.

The feed of external nuclei, also called primary particles is model by

$$\dot{n}_{\text{feed}} = \frac{\dot{N}_{\text{feed}}}{\sigma_{\text{feed}}\sqrt{2\pi}} \exp\left(-\frac{(v - v_{\text{feed}})^2}{2\sigma_{\text{feed}}^2}\right) \tag{11}$$

under the assumption the total number of feed particles $\dot{N}_{\text{feed}}$ is distributed normally around the nominal volume v_{feed}.

It is assumed that particles are withdrawn from the fluidization chamber without internal separation, i.e.,

$$\dot{n}_{\text{out}} = Kn, \tag{12}$$

where K denotes the withdrawal rate. The computation of K will be explained at the end of this section. The withdrawn particles are sieved externally using two sieves with opening diameters $L_1 > L_2$ in order to separate particle within the desired product size range $L_2 < L < L_1$ from over- and undersized ones. The non-ideal separation functions characterizing the sieves are modeled by cumulative Gaussian functions

$$\tilde{T}_i(L) = \frac{1}{\sigma_i\sqrt{2\pi}} \int_0^L \exp\left(-\frac{(\lambda - L_i)^2}{2\sigma_i^2}\right) \mathrm{d}\lambda\,, \quad i \in 1, 2 \tag{13}$$

where σ_i determines the selectivity of separation. By introducing Equation (1), the volume-dependent separation functions $T_1(v)$ and $T_2(v)$ are obtained. The fines particle fraction, given by

$$\dot{n}_{\text{under}} = (1 - T_1)(1 - T_2)\dot{n}_{\text{out}} \tag{14}$$

is fed back directly into the fluidization chamber without time delay for further size enlargement. The product fraction

$$\dot{n}_{\text{prod}} = (1 - T_1)T_2\dot{n}_{\text{out}} \tag{15}$$

is removed from the process, while the oversized fraction

$$\dot{n}_{\text{over}} = T_1\dot{n}_{\text{out}} \tag{16}$$

is milled into fine particles to serve as new nuclei. For simplicity it is assumed that the milled particles are distributed according to the Gaussian mill function

$$\tilde{q}_{0,\mathrm{mill}}(L) = \frac{1}{\sigma_{\mathrm{mill}}\sqrt{2\pi}} \exp\left(-\frac{(L - L_{\mathrm{mill}})^2}{2\sigma_{\mathrm{mill}}^2}\right) \tag{17}$$

with milling grade L_{mill} and variation σ_{mill}. From the number conservation the volume-based mill distribution is obtained as

$$q_{0,\mathrm{mill}}(v) = \tilde{q}_{0,\mathrm{mill}}(L)\frac{\mathrm{d}L}{\mathrm{d}v}. \tag{18}$$

The number density distribution of milled particles is obtained by equating the mass of oversized and milled particles [5,15]:

$$\dot{n}_{\mathrm{mill}} = q_{0,\mathrm{mill}} \frac{\int_0^\infty v\dot{n}_{\mathrm{over}}\,\mathrm{d}v}{\int_0^\infty v q_{0,\mathrm{mill}}\mathrm{d}v}. \tag{19}$$

From a practical point of view it is crucial to keep the total particle bed mass within certain boundaries in order to maintain the fluidization state. Hence, the system is described as a differential-algebraic system with the additional conservation equation

$$0 = m_{\mathrm{bed},0} - \rho_{\mathrm{p}} \int_0^\infty v n(t,v)\mathrm{d}v, \tag{20}$$

where $m_{\mathrm{bed},0}$ is the desired bed mass and ρ_{p} is the particle density. The integral term on the right-hand side describes the first moment of the particle size distribution and corresponds to the total particle volume in the fluidization chamber. Differentiating Equation (20) and inserting the PBE (2) yields the ideal withdrawal rate

$$K = \frac{\int_0^\infty v\left(\dot{n}_{\mathrm{growth}} + \dot{n}_{\mathrm{feed}}\right)\mathrm{d}v}{\int_0^\infty v\dot{n}_{\mathrm{prod}}\mathrm{d}v}, \tag{21}$$

compensating for the increase in bed mass by binder and external nuclei addition.

The model presented above has been validated without the agglomeration term and some small adjustments in e.g., Neugebauer et al. [5], the agglomeration process model has been validated experimentally but without recycle in Otto et al. [25].

3. Bifurcation Analysis

This section is concerned with the bifurcation analysis extending the results from Radichkov et al. [4], Dreyschultze et al. [6] and Neugebauer et al. [5] for the process with agglomeration. For the bifurcation analysis the DAE system defined by Equations (2) and (20) has to be solved numerically, typically achieved by application of a moment method [26] or the discretization of the volume coordinate [27,28]. In this contribution we choose the finite volume scheme presented in Singh et al. [28] which achieves high accuracy of the NDF compared to the moment methods and is straightforward to implement as well as numerically efficient compared to more complex discretization methods. The resulting N-dimensional system of ordinary differential equations is implemented in Matlab and solved using the build-in function *ode15s* for stiff DAE systems.

Since the aim of this contribution is to investigate the stability behavior of the process with layering growth and agglomeration, relevant bifurcation parameters have to be identified. Previous contributions have established the mean size of milled particles L_{mill} to be the most important variable regarding the occurrence of limit cycles in the process, therefore we adopt it as the first bifurcation parameter. In order to investigate the influence

of particle agglomeration it is recognized that the rate at which aggregation events between two granules occur is directly determined by the agglomeration efficiency β_0. The influence of other plant and process parameters is evaluated by investigating three samples in each case. The two-dimensional bifurcation analysis is reduced to a series of one-dimensional problems by discretizing β_0 logarithmically in the interval $[\beta_{0,\min}, \beta_{0,\max}]$. For every value of β_0 a parameter continuation [29] w.r.t. L_{mill} in the interval $[L_{\text{mill,min}}, L_{\text{mill,max}}]$ is conducted. The parameter continuation starts in the stable region with $L_{\text{mill}} = L_{\text{mill,max}}$, where the initial steady state NDF is obtained by solving the process model on the time interval $[0\text{h}, 100\text{h}]$. Afterwards L_{mill} is decreased by a small step ΔL and a prediction for the corresponding steady state is given using a tangent predictor [29]. The prediction is corrected by using it as initial guess for minimizing the sum of squares of the time derivatives by a Levenberg–Marquardt algorithm implemented in the Matlab function *lsqnonlin*. The procedure, where the NDF function is constrained to positive values, is repeated iteratively until $L_{\text{mill}} = L_{\text{mill,min}}$ is reached. In order to determine the stability of the steady state, the process model is linearized and eigenvalues are computed. In the case of at least one real part greater than zero, the corresponding steady state NDF is unstable and the existence of a stable limit cycle is tested by time integration. The bifurcation parameters are presented in Table 1.

Table 1. Parameters for the numerical bifurcation analysis.

Parameter	Min	Max	Number of Grid Points
β_0	$1 \times 10^{-14}\ \text{s}^{-1}$	$2 \times 10^{-14}\ \text{s}^{-1}$	42
L_{mill}	0.1 mm	0.8 mm	141

4. Results

As a basis for subsequent investigations, the stability analysis is carried out for the nominal case, where the plant and layering growth related parameters presented in Table 2 correspond to those given in Radichkov et al. [4], Dreyschultze et al. [6] and Bück et al. [30].

Table 2. (Nominal) simulation parameters.

Parameter	Value	Unit
N	200	-
$m_{\text{bed},0}$	100	kg
ρ_{p}	1600	$\text{kg}\,\text{m}^{-3}$
m_{inj}	100	$\text{kg}\,\text{h}^{-1}$
$\dot{m}_{\text{feed}}$	72	$\text{kg}\,\text{h}^{-1}$
L_{feed}	1	mm
σ_{feed}	0.15	mm
L_1	1.4	mm
σ_1	0.055	mm
L_1	1.0	mm
σ_2	0.065	mm
σ_{mill}	0.1	mm
L_{init}	1	mm
σ_{init}	0.1	mm

The stability plot for the nominal parameter case is presented in Figure 4. The mill grade interval is chosen as $L_{\text{mill}} \in [0.1, 0.8]$. Larger particles are already part of the product size interval and smaller particles are undesired since in a practical fluidized bed they might be removed form the chamber by the exhaust air. In the area colored white, one stable steady state solution exists while in the black area the PDE solution converges to a stable limit cycle around an unstable equilibrium. For $\beta_0 = \beta_{0,\min} = 1 \times 10^{-14}$, the amount of agglomeration events is negligibly small and the bifurcation results correspond to the

results presented for the layering growth only case in Radichkov et al. [4] and Dreyschultze et al. [6], where a zone of instability is limited by two supercritical Hopf-bifurcation points located at $L_{\text{mill}} = 0.2$ mm and $L_{\text{mill}} = 0.61$ mm. For increasing values of β_0 both bifurcation points are shifted towards smaller mill grades until the left one reaches its minimum mill grade value at $\beta_0 \approx 5.5 \times 10^{-13}$. Further increasing β_0, the two bifurcation points are moving towards each other and collapse at $\beta_0 \approx 8 \times 10^{-13}$. For even larger values of β_0 no self-sustained oscillations are observed.

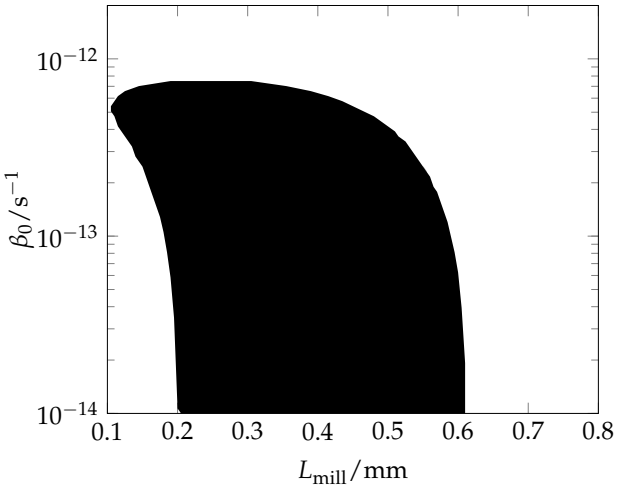

Figure 4. Stability map for the nominal parameter case. In the white region a stable steady states exists, in the black region an unstable stable steady state and a stable limit cycle exist.

In the following an explanation for the vanishing of the self-sustained oscillations with increasing agglomeration rates is developed. To this end, the oscillation of the NDF in the layering growth only case is described in three steps in accordance with Radichkov et al. [4]:

1. Beginning from a narrow particle size distribution, presented in Figure 5 (left), with a high fine particle mass fraction, the average particle diameter and the particle growth rate are small due to the high particle surface. Since the oversized mass fraction is small, a limited amount of particles is milled and only few new nuclei are formed. Therefore, the particle size distribution stays narrow.
2. Due to the particle growth the size distribution shifts towards larger particles and the average particle diameter rises. The fines mass fraction decreases while the product mass fraction increases (Figure 5, middle). Due to the narrow shape of the particle size distribution a large amount of particles reaches product size in a short time interval. Since the total bed mass is conserved only some of them are withdrawn and the particles grow further into the oversized range.
3. The oversized particles are withdrawn and milled and a large amount of new nuclei is formed in a short time interval (Figure 5, right). Since the total particle surface increases quickly the growth rate decreases accordingly and the narrow particle size distribution of the first phase is formed.

For the oscillation cycle described above it is crucial that the number density function stays narrow during the size enlargement, leading to two distinct "phases" where a uni-modal NDF either mainly grows or is mainly milled and fed back to form a new peak around the milling diameter. When L_{mill} is larger than the upper Hopf-bifurcation point, the oversized diameters and L_{mill} are too close for the emergence of distinct phases. For values of L_{mill} below the lower bifurcation point, the amount of new nuclei generated by the milling and the accordingly large total surface slow down the growth such that a large amount of particles can be withdrawn as product before reaching the oversized range. Thus, the formation of a second mode of nuclei is prevented and a stable equilibrium emerges.

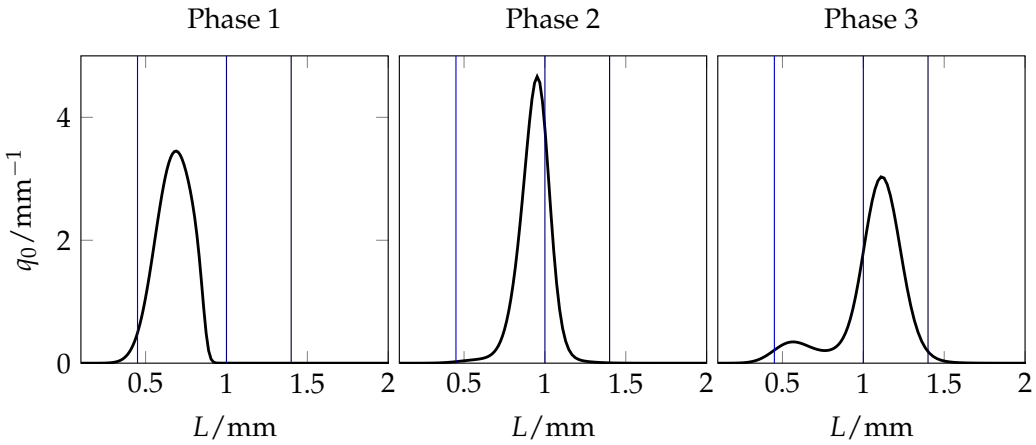

Figure 5. Normalized number density distributions $q_0(L)$ during the oscillation cycle described above with $L_{\mathrm{mill}} = 0.45$ mm. The vertical lines mark the milling diameter as well as the product and oversize sieve diameters.

In contrast to narrow particle size distributions, described above, wide particle size distributions can simultaneously grow in the small diameter region and be milled and fed back in the large diameter region leading to a flow equilibrium and therefore a stable distribution. It is well-known that the different mechanisms of layering growth and agglomeration promote narrow and wide size distributions, respectively. Due to the convection term describing the layering growth (6) the particle size distribution largely maintains its shape and only shifts to the right. The agglomeration term (9) however allows, depending on the specific agglomeration kernel, for the combination of two parent particles forming an agglomerate twice the volume quickly leading to a stretch of the initial number density function and therefore, in general, to a stabilization of the process dynamics. The larger the agglomeration efficiency is, the wider the NDF becomes. For $1 \times 10^{-13} < \beta_0 < 8 \times 10^{-13}$ and $L_{\mathrm{mill}} < 0.2$ mm however, agglomeration leads to the emergence of oscillations. In the granulation only case, the high total surface of milled particles slows down the growth and enables a stable equilibrium, here particle aggregation quickly reduces the particle surface and allows quick growth even if the milled particles are small.

In [11,31] the dynamics of a rotary drum granulation setup with sieve-mill recycle and size-enlargement due to layering and agglomeration have been investigated. The process model is quite similar to the present one, however an additional spatial coordinate along the rotational axis is introduced. Although no detailed bifurcation analysis with respect to the agglomeration efficiency has been conducted, self-sustained oscillations have been observed for process configurations where the milled particle size (crusher gap) is below some critical value. The proposed explanations are in accordance with the results presented above.

In the following, the influence of additional process and plant parameters on the occurrence and stability of equilibria is investigated. By varying the Kapur kernel parameters a and b the shape of the agglomeration kernel is changed. The agglomeration kernels depicted in Figure 6 show that an increase of the parameter b between $b = 0$ and $b = 0.3$ results in preferential agglomeration of small particles by increasing their agglomeration rate. The resulting bifurcation plots are presented in Figure 7, showing that the region of instability shrinks slightly. Since the variation of the parameter b increases the total agglomeration rate over all volumes, the results support the general finding that increased agglomeration dampens oscillations.

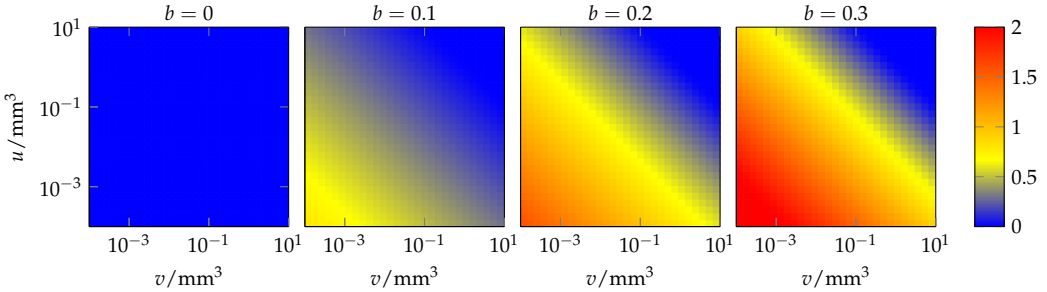

Figure 6. Agglomeration kernels $\beta(u, v)$ for variations of b. Colors indicate rate of agglomeration for different volume combinations.

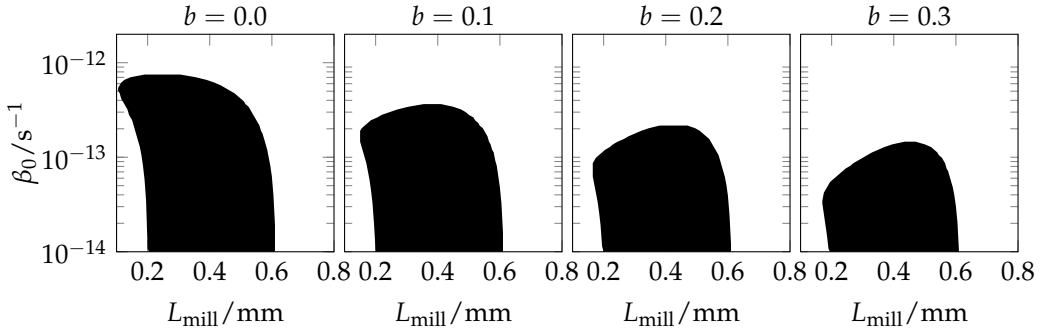

Figure 7. Stable (white) and unstable (black) regions for variations of b.

The layering growth rate G is directly proportional to the binder injection rate m_{inj}. Therefore, increasing the latter results in faster particle growth and more particles in the oversized fraction, preventing the formation of the stable equilibrium for mill diameters smaller than 0.2 mm due to the mechanism described above described above. Decreasing m_{inj} has the inverse effect as presented in Figure 8. The lower growth rate allows for the withdrawal of most particles in the product region, in turn minimizing the oversized fraction such that no new mode of milled particles is created.

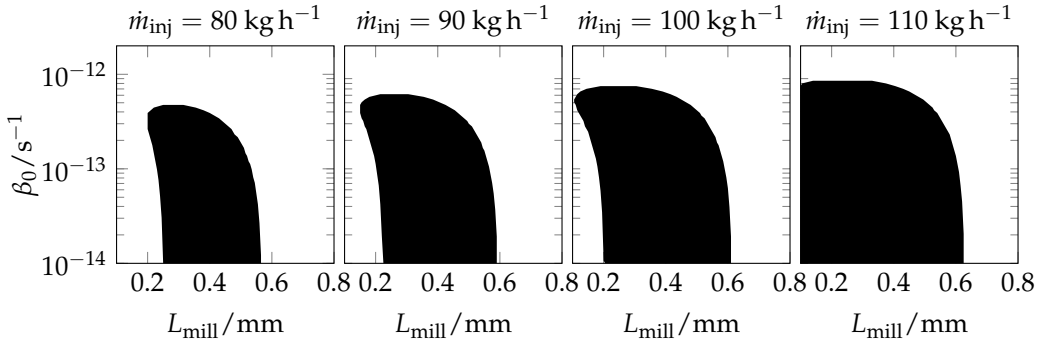

Figure 8. Stable (white) and unstable (black) regions for variations of the binder injection rate.

The feed of external nuclei creates new nuclei for agglomeration and layering. The main reason for the occurrence of self-sustained oscillations is that only few new nuclei are added in the "growing phase" and the NDF maintains its narrow shape. Therefore, reducing the number of new nuclei by decreasing the feed rate $\dot{m}_{\mathrm{feed}}$ promotes the occurrence of limits cycles and the expansion of the unstable region as presented in Figure 9.

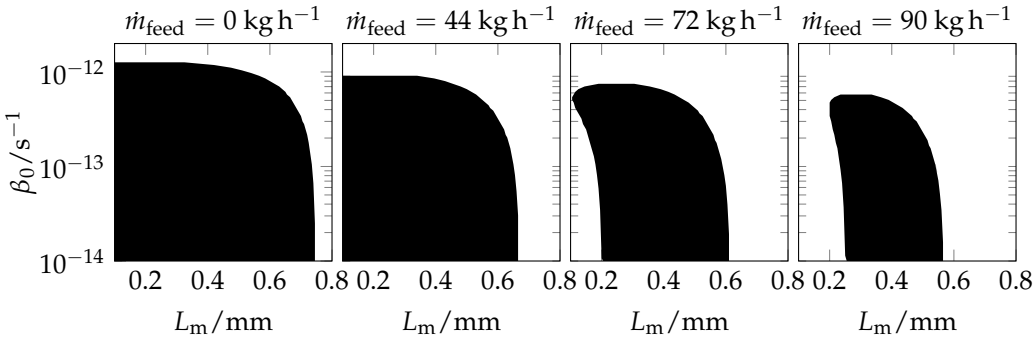

Figure 9. Stable (white) and unstable (black) regions for variations of the external particle feed rate.

The quality of the product particles is mainly determined by their average diameter and its variation which can be improved by varying the sieving diameter if required. Hence, a change of the sieve diameter L_2 around its nominal value $L_{2,\text{nom}} = 1$ mm is investigated and presented in Figure 10. It can be seen that, in general, larger values shift the unstable region towards larger mill diameters. Due to the reduced product size range, oscillations are possible for larger mill grades and the upper Hopf-bifurcation points are shifted to the right. On the other hand, the stable region left to the lower bifurcation points is also more pronounced. One reason for this might be the increased time span milled particles have before they reach product size allowing for the NDF to broaden by addition of external nuclei.

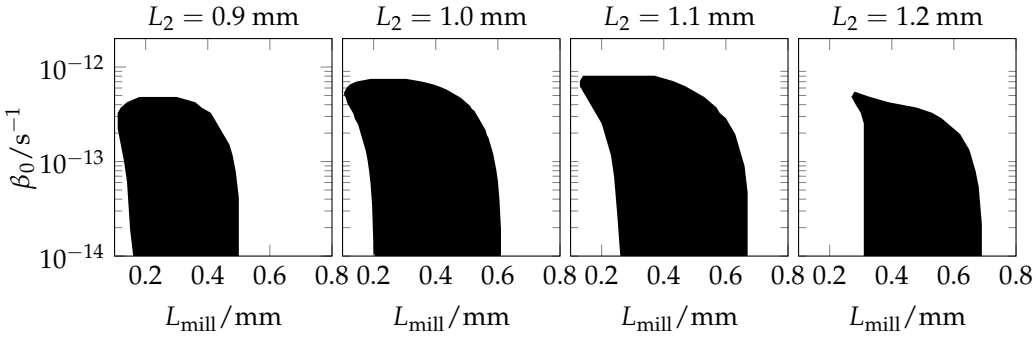

Figure 10. Stable (white) and unstable (black) regions for variations of the sieve diameter.

5. Conclusions and Outlook

The present contribution investigates the stability of a fluidized bed granulation process with particle size enlargement due to layering growth and agglomeration for a process configuration with sieve-mill-recycle. Based on the well-known occurrence of self-sustained oscillations in the number density function for pure layering growth, a numerical bifurcation analysis shows that the process exhibits no oscillations and only one stable steady state if the agglomeration rate is beyond a critical upper limit, independently of the milling parameters. If the process is operated below this limit, the application of stable process control is recommended. This result is obtained for different variations of additional process parameters such as agglomeration kernel parameters, binder injection rate, external particle feed rate and sieve diameters. It is worth noting, that similar results have been obtained in drum granulation with simultaneous agglomeration and layering [11]. The findings can be used as a basis for the design of a stable continuous process and show whether additional process control may be required for a constant quality product.

Future research directions may include the a refinement of the process model including additional particle properties such as porosity and the incorporation of a more detailed model for the agglomeration and layering growth kinetics. Furthermore, experimental confirmation of the predicted bifurcation phenomena development and implementation of sophisticated process control for the stabilization of unstable dynamics are of interest.

Author Contributions: Conceptualization, R.D. and A.K.; methodology, E.O.; software, E.O.; validation, E.O., R.D. and A.K.; data curation, E.O.; writing—original draft preparation, E.O.; writing—review and editing, R.D. and A.K.; visualization, E.O.; supervision, R.D. and A.K.; funding acquisition, A.K. All authors have read and agreed to the published version of the manuscript.

Funding: The financial support of the German Research Foundation (DFG) within the priority program SPP 2364 "Autonomous Processes in Particle Technology" under grant KI 417/10-1 is gratefully acknowledged.

Conflicts of Interest: The authors declare no conflict of interest. The funders had no role in the design of the study; in the collection, analyses, or interpretation of data; in the writing of the manuscript; or in the decision to publish the results.

Abbreviations

The following abbreviations are used in this manuscript:

PBE	population balance equation
NDF	number density function

Nomenclature

The following variables are used in this manuscript:

a	agglomeration kernel parameters	β_0	agglomeration efficiency
b	agglomeration kernel parameters	β	agglomeration kernel
m	mass	σ	standard deviation
$\dot{m}$	mass flow rate	ρ	density
n	volume-based number density function		
$\tilde{n}$	diameter-based number density function	1	lower sieve
q	normalized density function	2	upper sieve
t	time		
u	particle volume	agg	agglomeration
v	particle volume	growth	layering growth
		feed	particle feed
A	particle surface	fines	fine particles
G	volume-based growth rate	inj	binder injection
$\tilde{G}$	volume-based growth rate	max	maximum
K	withdrawal rate	mill	particle mill
L	particle diameter	min	minimum
N	number of discretization classes	out	particle outlet
$\dot{N}$	number flow rate	over	oversized particles
T	separation function	p	particle
		prod	product particle

References

1. Strenzke, G.; Dürr, R.; Bück, A.; Tsotsas, E. Influence of operating parameters on process behavior and product quality in continuous spray fluidized bed agglomeration. *Powder Technol.* **2020**, *375*, 210–220. [CrossRef]
2. Ennis, B.J.; Tardos, G.; Pfeffer, R. A microlevel-based characterization of granulation phenomena. *Powder Technol.* **1991**, *65*, 257–272. [CrossRef]
3. Rieck, C.; Bück, A.; Tsotsas, E. Estimation of the dominant size enlargement mechanism in spray fluidized bed processes. *AIChE J.* **2020**, *66*, e16920. [CrossRef]
4. Radichkov, R.; Müller, T.; Kienle, A.; Heinrich, S.; Peglow, M.; Mörl, L. A numerical bifurcation analysis of continuous fluidized bed spray granulation with external product classification. *Chem. Eng. Process. Process Intensif.* **2006**, *45*, 826–837. [CrossRef]
5. Neugebauer, C.; Diez, E.; Bück, A.; Palis, S.; Heinrich, S.; Kienle, A. On the dynamics and control of continuous fluidized bed layering granulation with screen-mill-cycle. *Powder Technol.* **2019**, *354*, 765–778. [CrossRef]
6. Dreyschultze, C.; Neugebauer, C.; Palis, S.; Bück, A.; Tsotsas, E.; Heinrich, S.; Kienle, A. Influence of zone formation on stability of continuous fluidized bed layering granulation with external product classification. *Particuology* **2015**, *23*, 1–7. [CrossRef]
7. Schmidt, M.; Rieck, C.; Bück, A.; Tsotsas, E. Experimental investigation of process stability of continuous spray fluidized bed layering with external product separation. *Chem. Eng. Sci.* **2015**, *137*, 466–475. [CrossRef]

8. Schmidt, M.; Bück, A.; Tsotsas, E. Experimental investigation of the influence of drying conditions on process stability of continuous spray fluidized bed layering granulation with external product separation. *Powder Technol.* **2017**, *320*, 474–482. [CrossRef]
9. Palis, S.; Kienle, A. Discrepancy based control of particulate processes. *J. Process Control* **2014**, *24*, 33–46. [CrossRef]
10. Otto, E.; Behrens, J.; Dürr, R.; Palis, S.; Kienle, A. Discrepancy-based Control of Particle Processes. *J. Process. Control* **2021**, *110*, 99–109. [CrossRef]
11. Vesjolaja, L.; Glemmestad, B.; Lie, B. Double-Loop Control Structure for Rotary Drum Granulation Loop. *Processes* **2020**, *8*, 1423. [CrossRef]
12. Palis, S. Control induced instabilities in fluidized bed spray granulation. *J. Process Control* **2020**, *93*, 97–104. [CrossRef]
13. Otto, E.; Dürr, R.; Kienle, A. Bifurcation analysis of combined agglomeration and layering granulation in fluidized bed spray processes. In *32nd European Symposium on Computer Aided Process Engineering*; Montastruc, L., Negny, S., Eds.; Computer Aided Chemical Engineering; Elsevier: Amsterdam, The Netherlands, 2022; Volume 51, pp. 691–696.
14. Ramkrishna, D. *Population Balances: Theory and Applications to Particulate Systems in Engineering*; Academic Press: Cambridge, MA, USA, 2000.
15. Heinrich, S.; Peglow, M.; Ihlow, M.; Henneberg, M.; Mörl, L. Analysis of the start-up process in continuous fluidized bed spray granulation by population balance modelling. *Chem. Eng. Sci.* **2002**, *57*, 4369–4390. [CrossRef]
16. Mörl, L.; Heinrich, S.; Peglow, M. Chapter 2 Fluidized bed spray granulation. In *Granulation*; Salman, A., Hounslow, M., Seville, J., Eds.; Handbook of Powder Technology; Elsevier Science B.V.: Amsterdam, The Netherlands, 2007; Volume 11, pp. 21–188.
17. Neugebauer, C.; Bück, A.; Kienle, A. Control of Particle Size and Porosity in Continuous Fluidized-Bed Layering Granulation Processes. *Chem. Eng. Technol.* **2020**, *43*, 813–818. [CrossRef]
18. Hulburt, H.; Katz, S. Some problems in particle technology: A statistical mechanical formulation. *Chem. Eng. Sci.* **1964**, *19*, 555–574. [CrossRef]
19. Terrazas-Velarde, K.; Peglow, M.; Tsotsas, E. Investigation of the Kinetics of Fluidized Bed Spray Agglomeration Based on Stochastic Methods. *AIChE J.* **2011**, *57*, 3012–3026. [CrossRef]
20. Otto, E.; Palis, S.; Kienle, A. Chapter Nonlinear Control of Continuous Fluidized Bed Spray Agglomeration Processes. In *Stabilization of Distributed Parameter Systems: Design Methods and Applications*; Springer International Publishing: Berlin/Heidelberg, Germany, 2021; pp. 73–87.
21. Narni, N.R.; Peglow, M.; Warnecke, G.; Kumar, J.; Heinrich, S.; Kuipers, H. Modeling of aggregation kernels for fluidized beds using discrete particle model simulations. *Particuology* **2014**, *13*, 134–144. [CrossRef]
22. Liu, L.X.; Litster, J.D. Population balance modelling of granulation with a physically based coalescence kernel. *Chem. Eng. Sci.* **2002**, *57*, 2183–2191. [CrossRef]
23. Cryer, S.A. Modeling agglomeration processes in fluid-bed granulation. *AIChE J.* **1999**, *45*, 2069–2078. [CrossRef]
24. Kapur, P. Kinetics of granulation by non-random coalescence mechanism. *Chem. Eng. Sci.* **1972**, *27*, 1863–1869. [CrossRef]
25. Otto, E.; Dürr, R.; Strenzke, G.; Palis, S.; Bück, A.; Tsotsas, E.; Kienle, A. Kernel identification in continuous fluidized bed spray agglomeration from steady state data. *Adv. Powder Technol.* **2021**, *32*, 2517–2529. [CrossRef]
26. Dürr, R.; Bück, A. Approximate Moment Methods for Population Balance Equations in Particulate and Bioengineering Processes. *Processes* **2020**, *8*, 414. [CrossRef]
27. Kumar, J.; Peglow, M.; Warnecke, G.; Heinrich, S. The cell average technique for solving multi-dimensional aggregation population balance equations. *Comput. Chem. Eng.* **2008**, *32*, 1810–1830. [CrossRef]
28. Singh, M.; Kumar, J.; Bück, A.; Tsotsas, E. A volume consistent discrete formulation of aggregation population balance equation. *Math. Methods Appl. Sci.* **2015**, *39*, 2275–2286. [CrossRef]
29. Seydel, R.U. *Practical Bifurcation and Stability Analysis*; Springer: New York, NY, USA, 1998.
30. Bück, A.; Neugebauer, C.; Meyer, K.; Palis, S.; Diez, E.; Kienle, A.; Heinrich, S.; Tsotsas, E. Influence of operation parameters on process stability in continuous fluidised bed layering with external product classification. *Powder Technol.* **2016**, *300*, 37–45. [CrossRef]
31. Vesjolaja, L.; Glemmestad, B.; Lie, B. Dynamic model for simulating transient behaviour of rotary drum granulation loop. *Model. Identif. Control A Nor. Res. Bull.* **2020**, *41*, 65–77. [CrossRef]